1 **Complex dissolved organic matter on the roof of the world – Tibetan DOM**
2 **molecular characteristics track sources, land use effects, and processing along the**
3 **fluvial-limnic continuum**

5 Philipp **Maurischat** [1,2] **,** Michael **Seidel** [3] **,** Thorsten **Dittmar** [3,4], Georg **Guggenberger** [1]

6 [1] Institute of Soil Science, Leibniz University Hannover, 30419 Hannover, Germany

7 [2] Institute of Biology and Environmental Sciences (IBU), Carl von Ossietzky University of Oldenburg,
8   26129 Oldenburg, Germany

9 [3] Institute for Chemistry and Biology of the Marine Environment (ICBM), Carl von Ossietzky University
10   of Oldenburg, 26129 Oldenburg, Germany

11 [4] Helmholtz Institute for Functional Marine Biodiversity at the University of Oldenburg (HIFMB), 26129
12   Oldenburg, Germany

13 **Correspondence to: Philipp Maurischat (philipp.maurischat@uni-oldenburg.de)**

14 **Keywords:** Non-metric multidimensional scaling (NMDS), Alpine pastures, Natural organic matter
15 (NOM), Land use controls, Molecular NOM composition, Fourier-transform ion cyclotron resonance
16 mass spectrometry (FT-ICR-MS)
17
18 **Funding:** This research is a contribution to the International Research Training Group "Geo-ecosystems
19 in transition on the Tibetan Plateau (TransTiP)", funded by Deutsche Forschungsgemeinschaft (DFG
20 grant 317513741 / GRK 2309). Funding for MS by Cluster of Excellence EXC 2077 "The Ocean Floor –
21 Earth's Uncharted Interface" (Project number 390741603).
22
23 **Conflict of interest:** No conflict of interest.

24   Abstract

25   The Tibetan Plateau (TP) is the world's largest and highest plateau, comprising the earth's biggest

26   alpine pasture system. It is sensitive to impacts of climate change and anthropogenic pressure. Carbon

27   cycling on the TP is influenced by glaciation and degradation of the pasture ecosystem. Dissolved

28   organic matter (DOM) connects carbon reservoirs, following the hydrological continuum from glaciers

29   and headwaters to lakes. Due to its complexity, DOM cycling along the aquatic continuum and the

30   impact of land use and climate change on DOM characteristics are still not well understood. Here, we

31   study solid phase extracted (SPE) DOM molecular characteristics using ultrahigh-resolution mass

32   spectrometry (FT-ICR-MS) along the TP hydrological continuum from glaciers, groundwater springs,

33   and wetlands including pastures and alpine steppes, to the endorheic Lake Nam Co. Our study revealed

34   that the SPE-DOM composition was largely influenced by local sources of glaciers, wetlands, and

35   groundwater springs as well as pasture degradation. Glacial meltwater SPE-DOM contained more

36   saturated compounds suggesting microbial sources together with aromatic compounds probably

37   derived from aeolian deposition. In comparison, wetland and stream SPE-DOM were characterised by

38   a higher percentage of highly unsaturated and aromatic molecular formulae. These were likely derived

39   from inputs of vascular plants and soils. Groundwater spring SPE-DOM from degraded pastures

40   differed from intact pasture samples. In degraded systems a strongly oxidised signature with lowest

41   counts of P heteroatoms, lower O/C ratio and higher aromaticity of SPE-DOM together with a high

42   degradation index suggested a strong transformation of SPE-DOM. SPE-DOM of the endorheic lake was

43   richer in unsaturated molecular formulae compared to the tributaries. This suggests algal and microbial

44   sources and production in the lake. The SPE-DOM rich in aromatic and highly unsaturated formulae

45   visible in the brackish zone of the lake shore contrasted sharply with the lake samples. Aromatic

46   molecular formulae were strongly depleted in the lake deep water indicating photooxidation of

47   riverine SPE-DOM. This shows that alpine SPE-DOM signatures are shaped by small-scale catchment

48   properties, land degradation, and the influence of glaciers and wetlands. The close link of alpine SPE-

49   DOM composition to landscape properties is indicative for a strong susceptibility of DOM

50   characteristics to climatic and land use changes in High Asia.
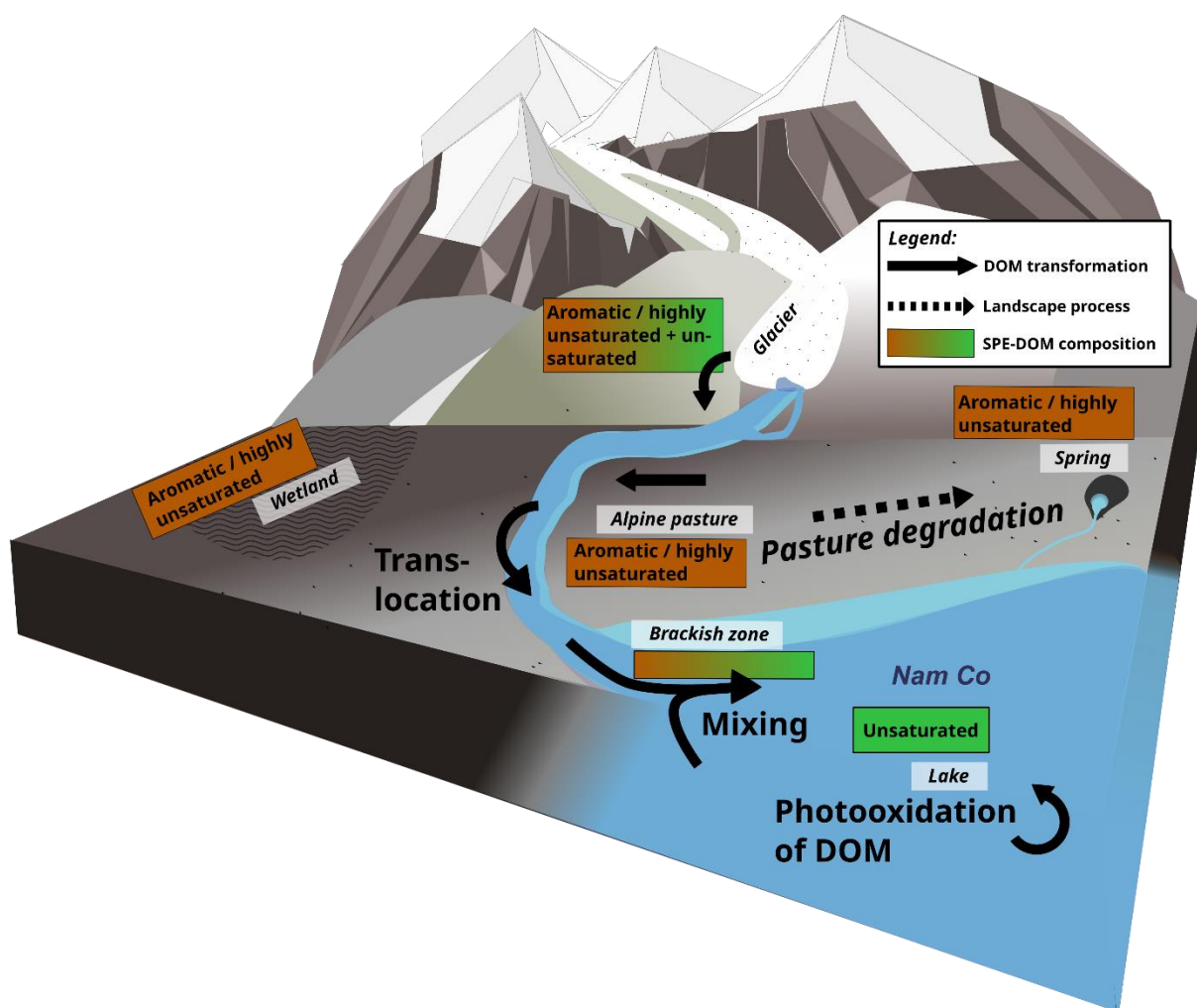
Graphical Abstract: Main processes shaping SPE-DOM molecular characteristics and transformations in the high-alpine Nam Co catchment. DOM processing and sources are indicated by black arrows. Pasture degradation is indicated by a dashed arrow.

1. Introduction

The Tibetan Plateau (TP) comprises the largest alpine pasture system in the world (Miehe et al., 2019) and is known as Asia's water tower (Bandyopadhyay, 2013), forming the source of large river systems. Large amounts of the water are stored in the ice masses of the TP, forming the largest frozen freshwater reservoir outside the polar regions. This third pole environment is well investigated (Qiu, 2008; Yao et al., 2012), revealing that High Asia's ecosystems are threatened (Hopping et al., 2018) by climate change (Yao, 2019) and by intensification of land use (Harris, 2010). Furthermore, emerging freshwater quality issues give reason for concern (Qu et al., 2019).

Nutrient and energy cycles of ecosystems are connected by dissolved organic matter (DOM) fluxes (Spencer et al., 2014). DOM can connect fluvial ecosystems over hundreds of kilometres (Seidel et al., 2015) and links terrestrial and aquatic ecosystems (Goodman et al., 2011). Biogeochemical processing

and DOM sources are known to shape the molecular composition of DOM (Liu et al., 2020; Roebuck et al., 2020; Seifert et al., 2016; Wilson and Xenopoulos, 2009). But how the DOM characteristics are influenced by different ecosystems and how DOM responds to ecosystem degradation is not well understood yet.

Fourier-transform ion cyclotron resonance mass spectrometry (FT-ICR-MS) is an ultrahigh-resolution method allowing the identification of thousands of molecular formulae, offering an opportunity to better understand molecular characteristics of solid-phase extracted (SPE) DOM, as well as sources, and transformations (Hawkes et al., 2020; Leyva et al., 2020; Šantl-Temkiv et al., 2013). Here we used FT-ICR-MS analysis to decipher characteristics and processing of stream SPE-DOM of different subcatchments, glaciers, a groundwater spring, an alpine wetland as well as SPE-DOM of an endorheic lake on the TP.

The Nam Co catchment, located in the southern part of the TP, lies in the transition zone of the *K. pygmaea* dominated alpine pasture ecosystem (Miehe et al., 2008) and the alpine steppe. The unique positioning in this transition zone is expressed between the south, with a more humid glacial-influenced high-mountain ecosystem contrasting the hilly northern margin of the catchment, with more arid climate and vegetation dominated by alpine steppe, where clear signs of pasture degradation are visible (Maurischat et al., 2022). This makes the Nam Co catchment a suitable natural laboratory to test for effects on organic matter (OM) characteristics and the cycling of OM in different ecosystems (Anslan et al., 2020). The effects of pasture degradation of Tibetan soils on OM stocks have been studied previously (Liu et al., 2017), but investigations on degradation induced changes of DOM composition have fallen short. Also, DOM characteristics and transformation in this complex natural interplay have only been investigated to limited extent. Spencer et al. (2014) found complex OM sources in glaciers, streams, and Lake Nam Co. A recent study highlighted a coupled decrease of "protein-like" DOM with an increase of "humic-like" DOM along the flow path (Li et al., 2021), whereas others found indications for less reactive stream DOM due to the cold and fast flowing water (Maurischat et al., 2022). This leaves important questions of 1) how DOM signatures are influenced by the diverse biotic and abiotic processes in the catchment with differing degrees of glaciation, alpine wetlands, and groundwater sources, as well as land degradation, and the alpine pasture alpine steppe ecotone, and 2) how DOM is processed along the streams and in the lake.

Our investigations aim at a better understanding of SPE-DOM processing at present conditions which will help to better understand the potential consequences of changing environmental conditions in the future. It is important to assess the potential vulnerability and responses of high-alpine ecosystems to anthropogenic changes. In this respect, we hypothesized:

99   I) SPE-DOM derived from different ecosystems (glaciers, groundwater springs and wetlands) and

100   streams in degraded land possess unique DOM signatures compared to the integrated DOM of

101   subcatchment streams.

102   II) The SPE-DOM transformation along the stream path is limited, no major compositional shift is

103   expected in-stream.

104   III) The SPE-DOM characteristics of lake water are chemically distinct from the terrestrial DOM sources

105   and integrated stream SPE-DOM composition.

106   2. Materials and methods

107   2.1 Site description and sampling

108   The Nam Co catchment has a total size of ~10800 km^2. Two main landscape units are distinguished, the

109   southern mountainous and the northern upland zone. The south of the catchment is characterised by

110   the Nyainqentanglha mountain ridge (NMR) with glaciation at highest elevations of more than 7000 m

111   asl. (Bolch et al., 2010). Glacial meltwater is the dominant water source of southern streams (Adnan

112   et al., 2019b). *K. pygmaea* pastures developed from 5300 m asl. downward (Anslan et al., 2020) and

113   are associated with a felty organic-rich topsoil (Kaiser et al., 2008). Closer to the lake alpine steppe

114   vegetation is prevailing (Nieberding et al., 2021). The southern part of the catchment is characterised

115   by higher precipitation compared to the north. Up to 530 mm y^{-1} are measured at the NMR (Anslan et

116   al., 2020). In the hilly uplands a less steep relief dominates (Yu et al., 2021), and an annual precipitation

117   of around 300 mm y^{-1} is reported (Anslan et al., 2020). Alpine pasture is developed in north-exposed

118   hill-flanks and valley bottoms, while alpine steppe grows on south exposed flanks, in the upland and

119   at the lake shoreline (Maurischat et al., 2022). Along with this aridity gradient from south to north,

120   land degradation is increasing (Anslan et al., 2020). The endorheic Lake Nam Co with an elevation of

121   4726 m asl. has a total size of ~2000 km². The lake is dimictic, oligotrophic, and lightly saline (0.9 g salt

122   l^{-1}; Keil et al., 2010) and has a depth of 99 m. It is well supplied with oxygen and has a clear water

123   column (Wang et al., 2020).

124   Three subcatchments of the Nam Co catchment were selected to represent the natural diversity (Fig.

125   1 a, b). The Niyaqu catchment (sample IDs 1:n in Fig. 1a, *low glaciation*) in the east has a total area of

126   406 km². Two streams drain the subcatchment, the southern stream receives meltwater from a glacier

127   of the NMR located 700 m above lake level. This river runs through extensive alpine pastures and feeds

128   a large alpine wetland (Fig. 1b, point 1:26). The northern stream drains a hilly upland area in the

129   transition of the alpine steppe and the alpine pasture. The herding of yaks takes place throughout the

130   year. The Zhagu subcatchment (sample IDs 3:n Fig. 1a, *no glaciation - degraded*) is located in the arid

131   north. It has a size of 46 km² and is mainly characterised by hilly upland relief (Keil et al., 2010). There

132 is no glacial influence and only a small altitudinal gradient in this catchment, with the highest elevation

133 at 5230 m. asl. Two creeks drain the catchment, both fed by groundwater springs. During sampling,

134 the streams were arheic, and clear signs of degradation of *K. pygmaea* pastures were visible

135 (Maurischat et al., 2022). Besides degraded pastures, alpine steppe is developed and used for animal

136 husbandry. In the south, the Qugaqie subcatchment (sample IDs 2:n Fig. 1b, *high glaciation*) represents

137 the NMR zone. The catchment has a size of 58 km² and is characterised by steep relief and a valley

138 course in south-north direction (Keil et al., 2010). The altitudinal difference between the lake and the

139 summit is 2200 m. This catchment is used as summer pasture.

140 Water samples were taken in September 2019 following the streams from source to terminus. Glaciers,

141 wetlands, and groundwater springs were sampled directly. Three source groups (glacial effluents,

142 groundwater springs, and alpine wetlands) and three sampling units (stream water, brackish water,

143 and lake water) were distinguished, resulting in six sample categories (Fig. 1). Glacial effluents were

144 drawn directly at or close to the glacial terminus, while groundwater was sampled directly at springs.

145 Alpine wetland samples were taken from the standing water column in the wetlands. Brackish water

146 samples were taken in the mixing zone of stream and lake water offshore in Lake Nam Co.

Data Source: JAXA ALOS World 3D - 30m (AW3030); Coordinate System: WGS 84/ UTM zone 46N EPSG: 3264; Landsat 5, 7, 8
imagery courtesy of the U.S. Geological Survey; Overview map: Data Commons License; openstreetmap.org (OSM)

147
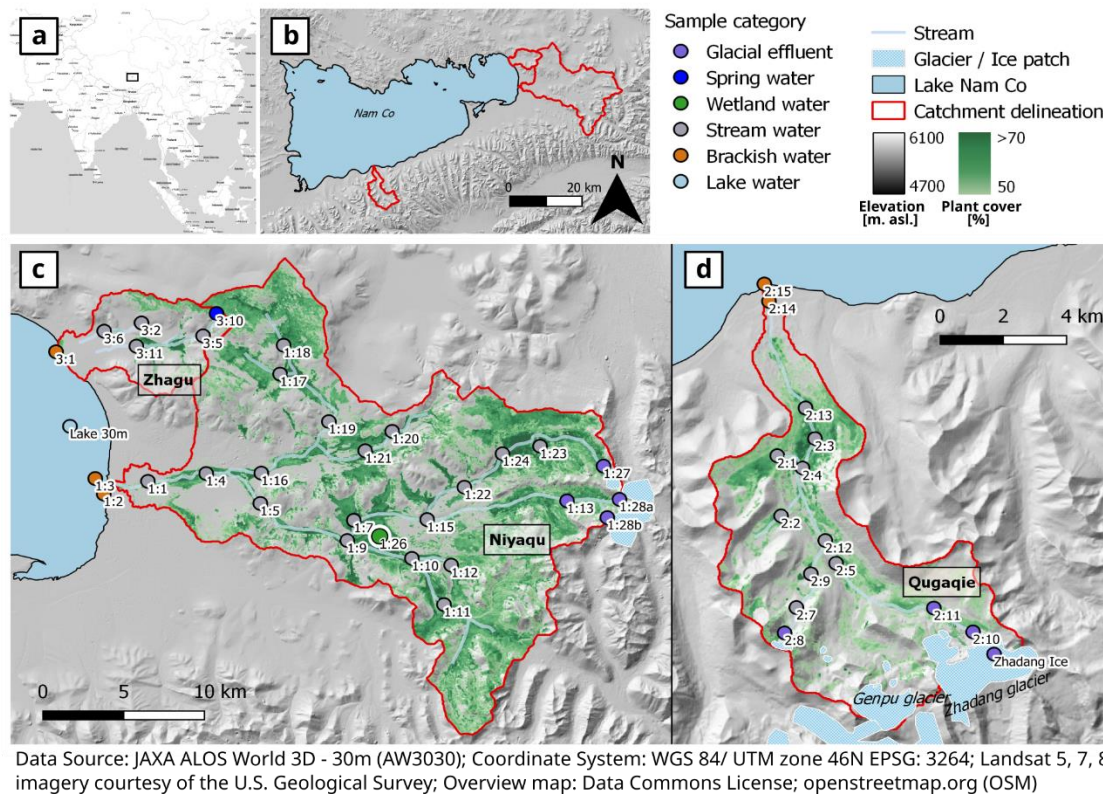
148 **Figure 1: (a) Overview map (Stamen Design, under CC BY 3.0. Data by Open Street Map contributors**
149 **2022, under CC BY SA, distributed under the Open Data Commons Open Database Licence, ODbL,**
150 **v1.0). The rectangle represents the sampling area. (b) Shows the outline of the Nam Co Lake and the**
151 **three subcatchments. (c) and (d) Map of the investigated subcatchments and sampling locations**

 with sample categories. Plant cover estimations from Maurischat et al. (2022) represent *K. pygmaea*
153 **pastures, the zones of most prominent yak grazing.**

154 Samples were taken from the middle of the stream profile using a telescopic sampling device. Lake
155 water was sampled from 30 m depth with a submersible sampler. All samples were taken in seven
156 subsamples with a volume of 1 L each, mixed and a 0.5 L aliquot of this was taken for analysis. Samples
157 were filtered on-site using a 0.45 µm mesh size polyethersulfone membrane (Supor, Pall, Port
158 Washington, USA), a filtration device and a portable electric pump. Samples were stored in pre-cleaned
159 high-density polyethylene bottles (Rotilabo, Carl Roth, Karlsruhe, Germany) and kept at -21°C until
160 analysis.

161 2.2 Solid-phase extraction

162 DOM samples were acidified to pH 2 using 32 % HCl (Rotipuran p.a., Carl Roth, Karlsruhe, Germany).
163 Dissolved organic carbon (DOC) concentrations were measured from 20 mL of sample by high-
164 temperature oxidation on a total organic carbon analyser (varioTOC Cube, Elementar, Langenselbold,
165 Germany). DOM samples were diluted with ultrapure water to a concentration of 1.5 mg C L^{-1}, 250 mL
166 of diluted sample were used for extraction. Cartridges with 100 mg of styrene divinylbenzene polymer
167 (PPL) resin (Bond Elut, Agilent Technologies, Santa Clara, USA) were used for extraction. SPE-DOM was
168 prepared following Dittmar et al. (2008). The SPE elute was transferred to cauterized brown glass flasks
169 (Neochrom, Neolab Migge, Heidelberg, Germany) sealed with polytetrafluorethylen caps (Neochrom,
170 Neolab Migge, Heidelberg, Germany) and stored at -18°C until analysis. The extraction efficiency was
171 evaluated by drying 0.2 mL of SPE-DOM under N_2 atmosphere and resolving the aliquot in ultrapure
172 water. The samples were then analysed for their DOC concentrations by high temperature oxidation
173 and the volumetric proportion of initial DOC to extracted SPE-DOC concentrations was calculated.
174 Reference material (Suwannee River / IHSS) (Green et al., 2015) was compared with routine assays.
175 Blank samples with ultrapure water were used to check for contamination.

176 2.3 Fourier-Transform Ion Cyclotron Resonance Mass Spectrometry

177 SPE-DOM samples were diluted in 1:1 methanol/ultrapure water to a final concentration of 5 mg C L^{-1}
178 for analysis. Samples were analysed in duplicates on a SolariX XR 15 Tesla FT-ICR-MS (Bruker Daltonik,
179 Bremen, Germany). Electrospray ionization (ESI) was carried out in negative mode and samples were
180 injected at a flow rate of 122 µL h^{-1}. 200 broadband scans (mass range of 92.14 to 2000 Da) were
181 acquired per sample, accumulation time was 0.2 s per scan. Mass spectra were internally calibrated
182 with a list of known $C_xH_yO_z$ molecular formulae over the mass range in the samples, achieving a mass
183 error of < 0.1 ppm. Instrument variability was assessed with an in–house standard of SPE-DOM from
184 North Equatorial Pacific Intermediate Water (NEqPIW) collected near Hawaii (Natural Energy

185   Laboratory of Hawaii Authority, NELHA) (Green et al., 2014). Molecular formula attribution was done

186   with ICBM-OCEAN (Merder et al., 2020). The method detection limit (MDL) was applied (Riedel and

187   Dittmar, 2014) with a minimum signal-to-noise ratio (S/MDL) of 2.5. Minimum signal to MDL ratio as

188   backbone for recalibration was 5 using mean recalibration mode. Molecular formulae were assigned

189   with a tolerance of 0.5 ppm as $C_{1-100}H_{1-125}O_{1-40}N_{0-4}S_{0-2}P_{0-1}$ in the mass range 95 to 1000 Da. Molecular

190   formulae assignments were accepted if the molecular formula was present in >5% of the samples.

191   Contaminants were identified and excluded using the contaminant reference mass list and in

192   additional conformity with the SPE-DOM process blanks. Detection limits for peaks were normalised

193   to sample peak intensities. The overall peak intensities were scaled to the local sample maxima using

194   the sum of peaks. Molecular formulae containing isotopes (^{13}C, ^{18}O, ^{15}N, ^{34}S) were removed from the

195   data table for further processing and molecular formulae with molar ratios of oxygen-to-carbon (O:C)

196   = 0, O:C ≥ 1, and hydrogen-to-carbon (H:C) > 2.5 were removed as well. Duplicate samples were

197   normalised, and molecular formulae were retained only when present in both duplicates.

2.4 SPE-DOM molecular descriptive classes, counts, and indices

199   Molecular formulae were assigned to SPE-DOM molecular compound classes (Leyva et al., 2020). The

200   original compound classification was taken from Šantl-Temkiv et al. (2013), and SPE-DOM compound

201   class labels were modified according to Merder et al. (2020). The modified aromaticity index (AI$_{mod}$)

202   representing SPE-DOM aromaticity, was calculated for each formula as proposed by Koch and Dittmar

203   (2006; 2016). AI$_{mod}$ > 0.5 was assigned as aromatic, while AI$_{mod}$ ≥ 0.67 was considered as condensed

204   aromatic compounds. The degradation index (I$_{Deg}$) was calculated as a measure of degradation state of

205   SPE-DOM (Flerus et al., 2012) and the terrestrial index (I$_{Terr}$) was calculated, as a measure of terrestrial

206   SPE-DOM sources (Medeiros et al., 2016). Molecular formulae that were part of the island of stability

207   (IOS) were evaluated to gain insight into the relative abundance of recalcitrant SPE-DOM (Lechtenfeld

208   et al., 2014). This is based on the assumption that the IOS contains SPE-DOM molecular formulae

209   representing recalcitrant oceanic SPE-DOM that is empirically stable on millennial time scales

210   (Lechtenfeld et al., 2014). The CHO index was calculated as a measure of organic carbon oxidation

211   (Mann et al., 2015). Low CHO values indicate highly reduced molecular formulae and high CHO values

212   indicate highly oxidised molecular formulae. Molecular diversity was interpreted as α-diversity by

213   depicting intracommunity molecular diversity (Thukral, 2017). Here we used the total number of

214   molecular formulae on the group scale of subcatchments and sample categories.

2.5 Statistical analyses

216   Molecular formula intensities were rescaled between 0 and 1. Grouping was conducted with two

217   independent factors: 1) the three subcatchments: Niyaqu (*low glaciation*), Qugaqie (*high glaciation*),

218   Zhagu (*degraded*) and Lake Nam Co; and 2) the sample categories: glacial effluents, spring, and wetland

219   as well as stream water, brackish water, and lake water. Samples from spring and wetland, as well as

220   Lake Nam Co, were excluded from statistical group comparisons due to the small sample sizes.

221   Intensity weighted arithmetic means, and standard deviations were calculated for AI_{mod}, number of

222   formulae containing the heteroatoms nitrogen (N), phosphorous (P) and sulphur (S), as well as the

223   total number of assigned formulae and for compound classes.

224   Due to violations of normal distribution and homoscedasticity in combination with unbalanced

225   sampling design, parametrical tests were considered unreliable (Bortz and Schuster, 2010). Multiple

226   pairwise comparisons were conducted using Kruskal-Wallis tests in combination with Bonferroni post

227   hoc corrected Dunn tests (Birnbaum, 1956). Significance levels of α = 0.05 were applied

228   (Supplementary material, Table S1 and Table S2).

229   Nonmetric multidimensional scaling (NMDS) was used for dimensionality reduction and ordination

230   (Anderson et al., 2006; Faith et al., 1987) based on a Bray-Curtis dissimilarity index matrix (k = 3). Data

231   for NMDS were scaled and mean-centred (Jolliffe, 2002). NMDS was performed for independent

232   factors (sites and sample categories), while those with low statistical power ($n < 3$) were not

233   incorporated. Loadings, scores, and R^2-coefficients of determination are provided in the

234   supplementary material (Tables S3 – S7). Co-correlation was checked visually and by Pearson's

235   correlation coefficient, defined as $|r| > 0.75$. The following compound classes were combined because

236   of co-correlation: aromatic O-rich and aromatic O-poor = ARO, highly unsaturated O-rich and highly

237   unsaturated O-poor = HUSAT, unsaturated O-rich, unsaturated O-poor and unsaturated with N = USAT

238   (Fig. 4). Collinear variables (section 2.6) were removed.

239   R software (The R project for statistical computing, v3.6.3, GNU free software) was used for statistics.

240   The R base packages (R Core Team, 2013) and *tidyverse* (Wickham et al., 2019) were used for data

241   organisation, pre-processing, and statistics. The packages *ggplot2* (Wickham et al., 2019) and *vegan*

242   (Oksanen et al., 2020) were used for graphical illustration and for NMDS analysis, respectively.

243   2.6 Environmental variables for statistical analysis

244   Several parameters were used as predictor variables in the NMDS. Internal predictor variables were

245   generated from the SPE-DOM dataset obtained by FT-ICR-MS (SPE-DOM indices, compound class

246   percentages and heteroatom counts; described in section 2.4). External predictor variables were taken

247   from a previous study of the same site and the same sampling campaign (Maurischat et al. 2022) and

248   tested for statistical correlations with this SPE-DOM dataset. The selected external variables showed

249   evidence as functional predictors in the prior study and are acknowledged as key parameters for DOM

250   characterisation in numerous applications. The variables included fluorescent DOM (FDOM)

251   components (here used as the product of co-correlated microbial and terrestrial-like FDOM

252 components) (Fellman et al., 2010), DOC concentrations (Eklöf et al., 2021), δ^{13}C of DOC (Guo et al.,

253 2006), dissolved inorganic carbon (DIC) concentrations, as a catchment geology parameter (Wang et

254 al., 2016), nitrate concentrations (NO$_3^-$) (Harms et al., 2016), and the mean plant cover at the sampling

255 point as land use indicator (Sankar et al., 2020).

3. Results

3.1 Sample treatment and quality assessment

258 SPE-DOM extraction efficiencies were 61.4 % ± 18.6 % (Supplementary material, Table S8). DOM

259 extraction efficiencies and the number of SPE-DOM molecular formulae (detected by FT-ICR-MS) were

260 only weakly correlated (R^2=0.08, $F_{(1, 43)}$ =5.144, β=-0.007, p=0.02) indicating that extraction efficiency

261 was not an important driver of molecular variability in our samples. Duplicate SPE-DOM process blanks

262 had below 1000 molecular formulae assigned and the Suwannee River / IHSS reference material had

263 ~3500. Minimum molecular formulae count to accept NOM samples was set to 2000, roughly in the

264 range of the number of molecular formulae expected from terrestrial aquatic samples (Seidel et al.,

265 2017; Spencer et al., 2014). The in house-control standard (NEqPIW SPE-DOM) was run repeatedly

266 during analysis (n = 38) to account for instrument variability. On average, 3558 (± 218) molecular

267 formulae were assigned: no significant instrument drift was detected (Supplementary material Figure

268 S1).

3.2 Molecular group counts and statistics

270 The number of assigned molecular formulae, here termed α-diversity, decreased in the order Qugaqie

271 (*high glaciation*) > Zhagu (*degraded*) > Niyaqu (*low glaciation*) > Lake Nam Co. Lake Nam CO SPE-DOM

272 had 50 % less assigned molecular formulae compared to the subcatchments (Table 1). SPE-DOM

273 samples from wetland and brackish environments had the highest numbers of assigned molecular

274 formulae (Table 2), compositional shifts in the H/C and O/C ratio of brackish and lake SPE-DOM are

275 displayed in Figure 6a with a zoom on *m/z* 371 to 371.3 (Fig. 6b).

276 Lake Nam Co SPE-DOM had relatively more N-containing molecular formulae compared to SPE-DOM

277 samples from the subcatchments (Table 2). The relative abundance of S-containing molecular formulae

278 was significantly lower in *low glaciation* Niyaqu compared to *high glaciation* Qugaqie SPE-DOM

279 (p=0.005). P-containing molecular formulae were enriched in the lake compared to SPE-DOM of the

280 subcatchments (Table 1, Table S1). N-containing molecular formulae were more abundant in wetland

281 water and brackish SPE-DOM samples, while groundwater spring SPE-DOM samples had the lowest

282 count. Glacial SPE-DOM had the highest relative abundances of S-containing molecular formulae.

283 SPE-DOM of Lake Nam Co had lower AI_{mod} and I_{Terr} values, compared to the subcatchments (Table 1).

284 For the sample categories, brackish SPE-DOM had higher I_{Terr} values but no significant differences were

285 observed (Table 2). The H/C ratios were highest in Lake SPE-DOM (Table 1) with significantly higher

286 relative numbers of hydrogen compared to Niyaqu (p=0.005). Additionally, the CHO index showed that

287 Lake SPE-DOM and SPE-DOM of the *high glaciated* Qugaqie catchment were less oxidized compared

288 to SPE-DOM of the *degraded* Zhagu catchment (p=0.042| statistically tested only for subcatchments).

289 Correspondingly, I_{Deg} values, were significantly higher for *degraded* Zhagu compared to the *glaciated*

290 Niyaqu and Qugaqie subcatchments SPE-DOM (p=0.0002). IOS values, indicative of recalcitrant SPE-

291 DOM with relatively long residence times, showed a significantly higher contribution in *degraded*

292 Zhagu and Lake Nam Co compared to *low glaciated* Niyaqu and *high glaciated* Qugaqie (p= 0.04, 0.05,

293 respectively| statistically tested only for subcatchments). For sample categories (Table 2), H/C ratios

294 were higher in glacial and lake SPE-DOM and the CHO index suggested less oxidized SPE-DOM in glacial

295 effluents and the lake compared to terrestrial sources (Fig. 5). Correspondingly highest I_{Deg} values were

296 observed in SPE-DOM of the brackish zone and in groundwater springs. The percentage of IOS values

297 increased in lake and groundwater springs compared to glacial effluents, indicating differences in the

298 contribution of recalcitrant SPE-DOM.

299 Compound classes (Fig. 2) give an overview of the composition of SPE-DOM. Largest differences among

300 the sites were found for aromatic classes. Lake Nam Co had 80 % less aromatic (O)-rich molecular

301 formulae compared to the subcatchments. The lake had only 5 % of the abundance of aromatic O-poor

302 compounds compared to subcatchment SPE-DOM. For highly unsaturated O-rich molecular formulae,

303 Lake Nam Co had higher values compared to subcatchment SPE-DOM, while highly unsaturated O-

304 poor molecular formulae decreased in the lake. Furthermore, the unsaturated O-poor and unsaturated

305 N-containing SPE-DOM compounds were higher in lake SPE-DOM compared to the terrestrial systems.

306 Highly unsaturated O-rich formulae were more abundant in SPE-DOM of *high glaciation* Qugaqie

307 compared to *low glaciation* Niyaqu (Fig. 2).

Table 1: Overview on mean and standard deviation of indices and elemental composition ratios and mean and standard deviation of molecular formulae counts for sites.

Variable	Niyaqu (*low glaciation*) n=26		Qugaqie (*high glaciation*) n=15		Zhagu (*degraded*) n=4		Lake Nam Co ‡ n=1
	Mean	*SD (±)*	*Mean*	*SD (±)*	*Mean*	*SD (±)*	*Value*
AI_{mod}	0.33 [a]	0.05	0.32 [a]	0.02	0.36 [a]	0.02	0.25
O/C	0.46 [a]	0.02	0.45 [a]	0.02	0.45 [a]	0.02	0.44
H/C	1.12 [a]	0.08	1.17 [b]	0.05	1.13 [a,b]	0.08	1.20
CHO	-0.21 [a,b]	0.11	-0.26 [b]	0.08	-0.17 [a]	0.04	-0.29
I_{Deg}	0.55 [a]	0.15	0.59 [a]	0.10	0.77 [b]	0.02	0.33
I_{Terr}	0.32 [a]	0.13	0.35 [a]	0.03	0.34 [a]	0.04	0.08
IOS [%]	14.4 [a]	1.7	14.7 [a]	1.6	18.0 [b]	2.2	17.2
Number of formulae containing N	1412 [a] (49.2)	941	1928 [a] (54.9)	1083	1933 [a] (56.5)	951	1284 (58.8)
Number of formulae containing P	143 [a] (4.9)	112	129 [a] (3.6)	96	130 [a] (3.8)	54	196 (8.9)
Number of formulae containing S	69 [a] (2.4)	96	146 [b] (4.1)	101	46 [a,b] (1.3)	43	37 (1.6)
Total number of molecular formulae (α-diversity)	2867 [a]	1060	3509 [a]	1340	3416 [a]	848	2183

[a, b] Significant differences (α=0.05) are indicated by superscript letters. ‡ Single sample, standard deviations were not calculated and statistical tests were not performed. For heteroatoms (N, P, S), percentages of the total number of molecular formulae are given in parentheses. Boxplots of data are presented in the supplementary material (Fig. S2).

Table 2: Overview on mean and standard deviation of indices and elemental composition ratios and mean and standard deviation of formulae counts for sample categories.

Variable	Glacial effluent n=8		Spring ‡ n=1	Wetland ‡ n=1	Stream water n=38		Brackish water n=4		Lake water ‡ n=1
	Mean	*SD (±)*	*Value*	*Value*	*Mean*	*SD (±)*	*Mean*	*SD (±)*	*Value*
AI_{mod}	0.31 [a]	0.04	0.35	0.33	0.33 [a]	0.05	0.35 [a]	0.02	0.25
O/C	0.45 [a]	0.03	0.44	0.46	0.46 [a]	0.02	0.46 [a]	0.01	0.44
H/C	1.17 [a]	0.08	1.15	1.09	1.13 [a]	0.07	1.13 [a]	0.07	1.20
CHO	-0.28 [a]	0.14	-0.18	-0.19	-0.22 [a]	0.09	-0.18 [a]	0.07	-0.29
I_{Deg}	0.53 [a]	0.13	0.77	0.53	0.58 [a]	0.15	0.66 [a]	0.02	0.33
I_{Terr}	0.34 [a]	0.06	0.32	0.34	0.32 [a]	0.11	0.39 [a]	0.04	0.08
IOS [%]	13.7 [a]	2.24	17.4	16.0	15.1 [a]	1.9	14.5 [a]	1.33	17.2
Number of formulae containing N	1548 [a] (52.2)	1135	1261 (44.7)	2549 (62.3)	1511 [a] (44.2)	922	2586 [a] (57.5)	1231	1284 (58.8)
Number of formulae containing P	103 [a] (3.4)	90	117 (4.1)	291 (7.1)	130 [a] (3.8)	91	231 [a] (5.1)	160	196 (8.9)
Number of formulae containing S	134 [a] (4.5)	125	9 (0.3)	68 (1.6)	77 [a] (2.2)	90	163 [a] (3.6)	126	37 (1.6)
Total number of formulae (α-diversity)	2965 [a]	1132	2819	4091	3416 [a]	1053	4492 [a]	1639	2183

a, b Significant differences (α=0.05) are indicated by superscript letters. ‡ Single sample, standard deviations were not calculated and statistical tests were not performed. For heteroatoms (N, P, S), percentages of the total number of molecular formulae are given in parentheses. Boxplots of data are presented in the supplementary material (Fig. S3).
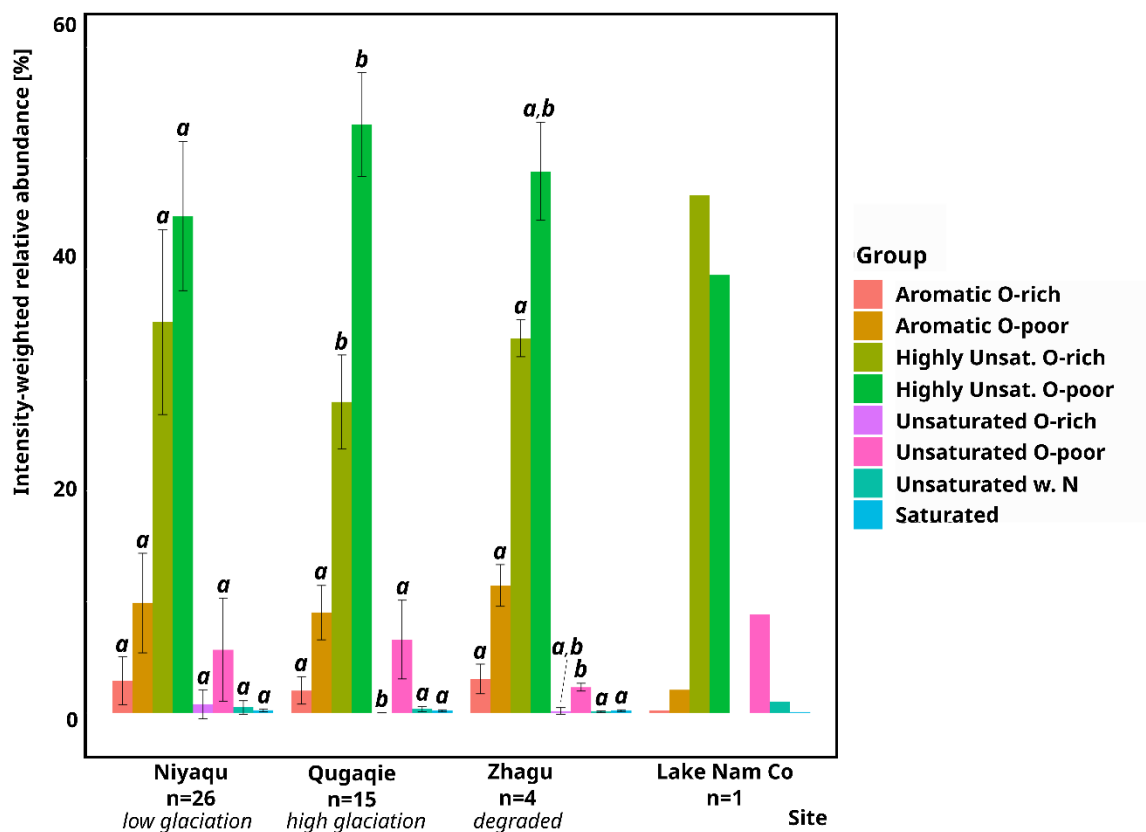
Figure 2: Relative intensity-weighted averages of SPE-DOM compound classes for stream water of the three subcatchments and Lake Nam Co (sites). For sample sizes n<3, no standard deviations are given. Error bars indicate standard deviations, significant differences (α=0.05) are indicated by superscript letters (a, b).

The relative abundances of aromatic compounds were different between lake SPE-DOM and SPE-DOM assigned to other sample categories, with samples from Nam Co having the lowest relative abundances (Fig. 3). Brackish SPE-DOM had significantly more aromatic O-poor compounds compared to glacial effluents (p=0.05). SPE-DOM from the Nam Co Lake had the highest relative abundances of highly unsaturated O-rich compounds compared to all other groups, especially glacial SPE-DOM had on average 40% less O-rich compounds.

331 Unsaturated O-poor compounds were relatively more abundant in lake SPE-DOM and glacial effluents

332 compared to the other environmental sample categories; this class was especially depleted in spring

333 SPE-DOM. Alongside Lake and glacial SPE-DOM were relatively rich in unsaturated N-containing

334 formulae. Spring water had the fewest of this compound class (Figure 3).
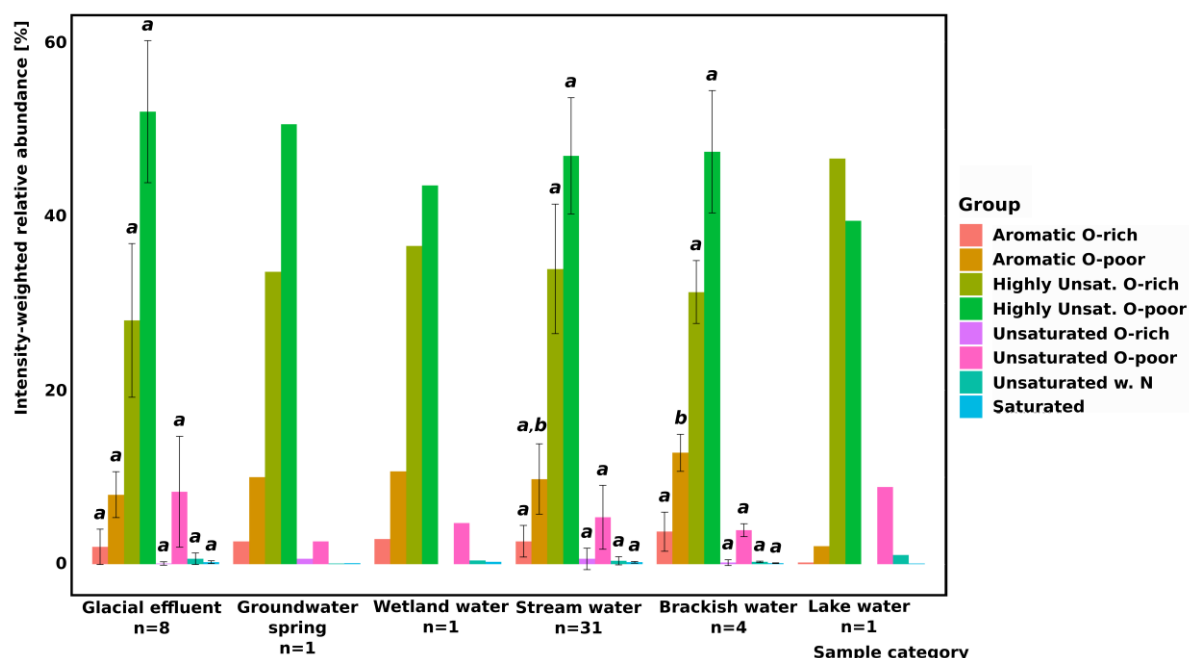
Figure 3: Relative intensity-weighted averages of DOM compound classes according to environmental sample categories. Error bars indicate standard deviations. For sample sizes n<3, no standard deviations are given. Error bars indicate standard deviations, significant differences (α=0.05) are indicated by superscript letters (a, b).

335 3.3 Multivariate statistical analysis

336 NMDS was conducted with a graphical overlay for sites and sample categories. The stress value of 0.14

337 is within tolerance (< 0.2; Dexter et al., 2018). In NMDS ordination (Fig. 4a) molecular formulae

338 expanded in the ordination plane above the coordinate origin. Samples were distributed in two groups

339 depending on aromaticity and related indicators (AI_{mod}, I_{Deg}, and I_{Terr}). AI_{mod} values increased from the

340 positive to the negative direction of the first dimension. In the positive direction of dimension 1,

341 samples containing relatively more unsaturated and saturated SPE-DOM compound classes as well as

342 S-containing compounds were distributed (Fig. 4b) these samples also had lower AI_{mod}, I_{Deg}, and I_{Terr}. In

343 the negative direction of dimension 1, samples with a higher abundance of aromatic compound classes

344 were distributed. The external predictors DIC and plant cover were loading in this direction along with

345 DOC concentrations and values of FDOM and $\delta^{13}C$ of DOM (black vectors in Fig. 4b) suggesting that

346 these samples were influenced by DOM inputs of plants and soils. The second dimension of the NMDS

347 ordination separated samples according to the abundance of highly unsaturated and saturated SPE-

348 DOM compounds, together with the N, P and S heteroatoms. These samples were also characterized

349 by elevated NO_3 concentrations. Samples located closer to the origin of predictor variable vectors were

350 related to higher IOS percentages and suggested a higher abundance of recalcitrant SPE-DOM.

351 Samples of the *degraded* Zhagu subcatchment were located close to the centre of predictor variable

352 vectors (Fig. 4b), while samples of *high glaciation* Qugaqie were scattered on the dimension plane.

353 SPE-DOM from the *low glaciation* Niyaqu subcatchment as more uniformly placed in the lower part.

354 Stream water SPE-DOM was scattered, indicating large chemical diversity. Most brackish SPE-DOM

355 samples were placed in the upper left of the plane, associated with higher terrestrial indicators (AI_{mod},

356 I_{Deg}, and I_{Terr}) and more abundance of N and P heteroatoms. Glacial SPE-DOM was associated with

357 heteroatoms, saturated and unsaturated molecular compounds, and less depleted δ ^{13}C of DOM,

358 visible by its positioning in the bottom left to top right of the ordination plane.

4. Discussion

4. 1 Catchment properties shape SPE-DOM composition at Lake Nam Co

361 The subcatchments (*high glaciation, low glaciation and degraded*) of Lake Nam Co differed significantly

362 in their molecular SPE-DOM composition. The *high glaciation* subcatchment had the largest molecular

363 α-diversity and a larger abundance of S heteroatoms (Table 1). This can be influenced by the

364 productivity of the glacial ecosystem (Hodson et al., 2008). S heteroatoms in DOM are likely related to

365 high sulphide contents in the runoff of Zhadang glacier (Yu et al., 2021). Sulphate reduction takes place

366 in glacial sediments and ice (Wu et al., 2012). Under sulfidic conditions, sulphide can be incorporated

367 into DOM ("sulfurization") (Pohlabeln et al., 2017). The higher abundance of O-poor compounds,

368 namely with depleted unsaturated O-rich and highly unsaturated O-rich molecular formulae and

369 increased highly unsaturated O-poor and unsaturated O-poor formulae alongside with negative CHO

370 values, indicates less intensively microbial transformed SPE-DOM compounds (Anesio et al., 2009;

371 Hood et al., 2009; Spencer et al., 2014) compared to the *degraded* and *low glaciation* subcatchments.

372 Accordingly, D'Andrilli et al. (2019) observed the relative increase of O-enriched molecular formulae

373 after bio-incubations of DOM. Likely, low water temperatures of the glacial meltwater in Qugaqie

374 hamper the microbial decomposition of DOM (Adams et al., 2010).
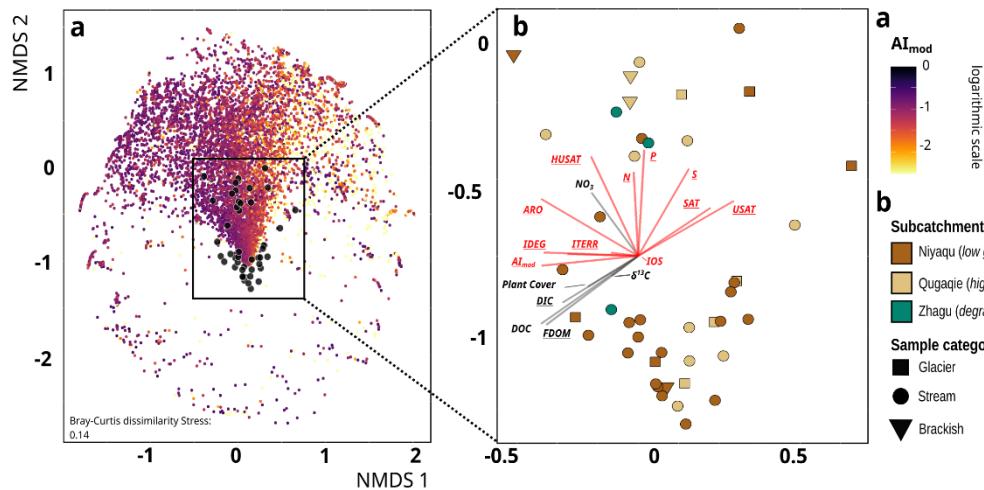
Figure 4: Non-metric multidimensional (NMDS) scaling analysis based on the relative abundances of SPE-DOM molecular formulae (calculated on Bray–Curtis dissimilarity matrix) (a) with the colour-coded modified aromaticity index (AI$_{mod}$, logarithmic scale) (Koch and Dittmar 2006; 2016). b) Zoom of NMDS analysis based on the relative abundances of SPE-DOM molecular formulae with post-hoc fitted SPE-DOM parameters (internal predictor variables, red) and environmental parameters (external predictor variables, black) shown as vectors. Underlined parameters were significantly ($p \leq 0.05$) related to NMDS ordination (stress = 0.14, k = 3). ARO= aromatic O-rich and aromatic O-poor, HUSAT= highly unsaturated O-rich and highly unsaturated O-poor, USAT= unsaturated O-rich, unsaturated O-poor and unsaturated with N, and SAT= saturated. Subcatchments are represented by the colour of sample points, while sample categories are represented by shapes.

Compared to the Qugaqie catchment, the contribution of glacial meltwater was smaller in the Niyaqu subcatchment and absent in Zhagu. The main water sources for Zhagu are precipitation and groundwater (Adnan et al., 2019a; Anslan et al., 2020; Tran et al., 2021). In the *degraded* Zhagu subcatchment, a stronger indication of aromaticity with higher AI$_{mod}$ and higher relative abundance of aromatic compounds was found. Likewise, the higher oxidation state indicated by the CHO index (Fig. 5b, Table 2) and higher degradation index (I$_{Deg}$, Table 2) suggest a larger share of soil-borne, aromatic DOM compounds This was also corroborated by the higher percentage of the IOS (+ ~3 %), indicating a larger input of degradation products. The *low glaciation* Niyaqu catchment in comparison had a higher contribution of aromatic and unsaturated compounds together with a lower H/C ratio, suggesting less oxidised DOM. In combination with the AI$_{mod}$ and I$_{Terr}$ indices this suggests inputs of soils and plants, including lignin and hemicellulose and their degradation products (Roebuck et al., 2018; Seifert et al., 2016).

The *high glaciation* Qugaqie catchment comprises of a signature rich in highly unsaturated O-poor and unsaturated O-poor formulae likely derived from a glacial-borne microbial source. Furthermore, the high aromatic indices (AI$_{mod}$, I$_{Terr}$) and high percentages of aromatic compound classes are indicative of SPE-DOM derived from soil and plant material. Likely, there is a steady input of soil-derived material into the streams from pastoral land as demonstrated for other grassland systems (Seifert et al., 2016;

403 Lu et al., 2015). Notably, this influence became smaller, when glacial-borne more unsaturated DOM
404 was more dominant on subcatchment level (Fig. 3b).

405 ## 4.2 The effect of pasture degradation on SPE-DOM composition

406 Molecular α-diversity defined by the number of molecular formulae and SPE-DOM characteristics can
407 be pinpointed to landscape units and environmental sample categories (summarized in Fig. 7). Glacial
408 SPE-DOM from Qugaqie and Niyaqu subcatchments contained two different signatures from different
409 sources. The first signature was characterized by high abundances of unsaturated compounds with and
410 without nitrogen as well as a low oxidation state of carbon (Fig. 5a), high ratios of H/C and low
411 percentages of recalcitrant SPE-DOM visible by the IOS. These parameters indicate relatively fresh,
412 reduced (oxygen-poor) SPE-DOM of low-molecular mass probably derived from microbial activity at
413 the partly anoxic ice shield. This is in-line with findings from other glacial environments worldwide
414 (Hood et al., 2009; Telling et al., 2011; Anesio et al., 2009). The second DOM signature was
415 characterized by aromatic and highly unsaturated compound classes, with aromatic and terrestrial
416 indices (I_{Terr}, AI_{mod}) suggesting plant- and soil-borne SPE-DOM sources, despite the absence of plant
417 cover in the glacial zones. Glaciers receive compounds with higher molecular mass from aeolian
418 deposition, either condensed (poly)aromatics, e.g. from the burning of fossil fuels (Takeuchi, 2002) or
419 compounds uncondensed but rich in phenolics, usually associated with dust from degraded vascular
420 plant material and soils (Singer et al., 2012). Local dust formation on the TP is projected to increase
421 with ongoing pasture degradation (Wang et al., 2008), likely affecting the DOM composition of glaciers.
422 The coexistence of microbially produced, autochthonous DOM and airborne aromatic, allochthonous
423 DOM renders the understanding of the downstream fate of glacial DOM difficult.

424 Groundwater spring SPE-DOM from the *degraded* Zhagu subcatchment mainly contained aromatic and
425 highly unsaturated compounds. Molecular α-diversity and the number of N, P and S heteroatoms were
426 low. Together with the high I_{Deg} and CHO indices, this suggested a strong degradation of spring SPE-
427 DOM (Fig. 5b). Furthermore, 17% of DOM being IOS compounds indicated a large contribution of
428 recalcitrant DOM. Spring water is generally expected to inherit aquifer and catchment characteristics
429 in its DOM signature, also partly preserving its terrigenous source (Osterholz et al., 2022; Yoo et al.,
430 2020). The shallow groundwater table of Zhagu (Tran et al., 2021), is in contact with soil OM and yak
431 faeces (Maurischat et al., 2022), which can leach soil-borne OM to the groundwater (Connolly et al.,
432 2020) which re-emerge at groundwater springs. Hence, the highly degraded SPE-DOM compounds
433 likely originated from the degraded pedosphere and have been transported with the groundwater.
434 The connection of degraded pastures of Zhagu (Fig. 1 & 4b) with the molecular composition of
435 groundwater spring SPE-DOM indicates that highly modified DOM signatures are transported with the
436 spring water and retrieved in streams.

SPE-DOM of an alpine wetland had a high α-diversity (>4000 molecular formulae), was rich in N, and P heteroatoms, as well as in highly unsaturated O-rich, and unsaturated O-poor compounds. The wetland was also enriched in ammonium and DOC compared to the streams (Maurischat et al., 2022). Alpine wetlands are highly productive and contain large amounts of nutrients in biomass and soil OM (Bai et al., 2010; Zhang et al., 2020). Wetlands on the TP have been massively degrading (Zhang et al., 2011), enhancing microbial decomposition in wetland mire soils (Ma et al., 2018) and driving a subsequent release of nutrients into adjacent streams (Gao, 2016). For Nam Co Lake, this would pose a severe biodiversity threat to oligotrophic streams and the sensitive lake shore (Hu et al., 2016).

Stream samples are concentrated in the lower centre of the NMDS (Fig. 4b). These samples had a dominance of aromatic compounds either associated with highly unsaturated O-poor or highly unsaturated O-rich formulae, suggesting mostly inputs of terrestrial compounds, such as lignin and tannin and their degradation products (Mann et al., 2015), further corroborated by depleted δ^{13}C DOC signatures (Fig. 4b; Maurischat et al., 2022). The *K. pygmaea* ecosystem spreads as an azonal pasture along the streams (Fig. 1). Lu et al. (2015) pointed out that grassland sites provide terrestrial inputs of aromatic and highly unsaturated compounds to surface waters. The *K. pygmaea* pasture browsed by yak has potential influence of their faeces (Du et al., 2021), suggesting lower molecular mass and negative CHO inputs due to the reductive conditions in the yak gastrointestinal tract and decomposition of plant-borne material therein (Fahey et al., 1983). Stream samples can therefore also be under influence of changing inputs from the pasture ecosystem. Faeces inputs and products of their microbial utilisation are likely associated with increases of N-containing unsaturated formulae and saturated formulae (Vega et al., 2020). Pastoral land-use and pasture degradation both had a considerable impact on stream SPE-DOM composition. While intact pastures released a highly unsaturated and aromatic signature related to the pasture soils and plants, streams close to degraded pastures were characterised by highly oxidized aromatic signatures and low molecular α-diversity.

461
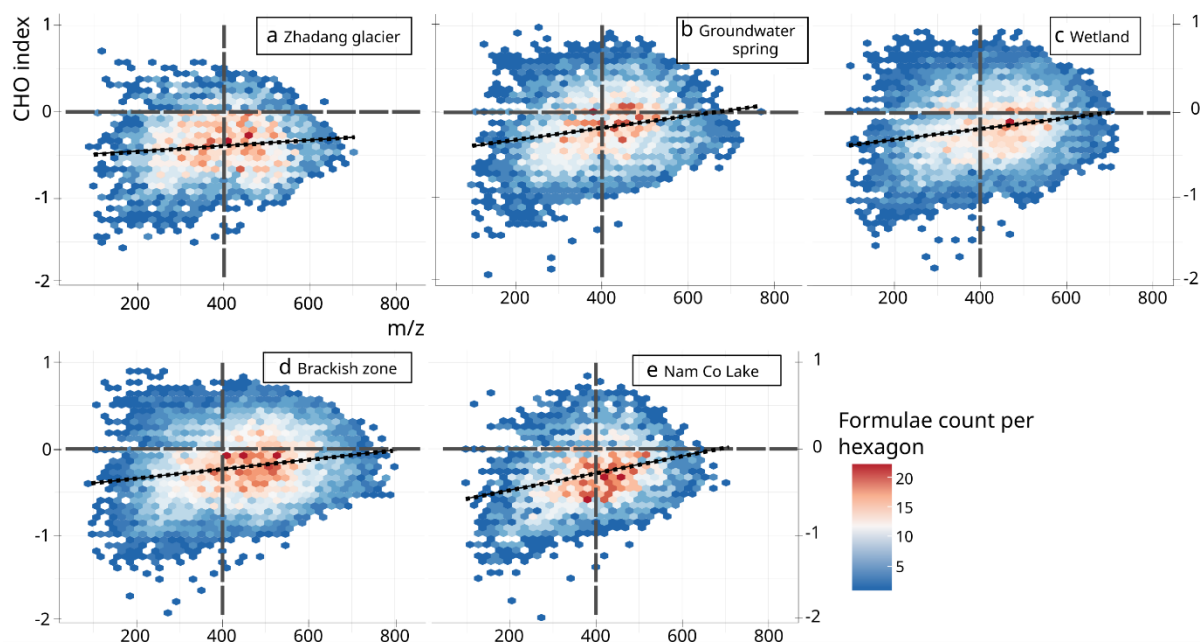
Figure 5: Hexagon scatters plot the count of the chemical formula in the space of the CHO index (Mann et al., 2015) and *m/z*. The black dotted lines represent the linear model of the CHO index and *m/z* of the respective sample, and the grey dashed lines split the plot into quadrants for orientation. The regression and ledger lines are printed to guide the eyes only. a) Ice from a glacier in *high glaciation* Qugaqie, b) groundwater spring from the upland of *degraded* Zhagu (3:10), c) water from the standing water column of a wetland (1:26), d) water from the brackish zone of Lake Nam Co and a tributary stream (2:15) and e) water sample from 30 m depth of Lake Nam Co. Axis scales are fixed.

4.3 The Lake reactor: photooxidation changes the SPE-DOM molecular composition

Brackish SPE-DOM samples had the highest molecular α-diversity, highest number of N and S heteroatoms and highest number of aromatic O-poor compounds together with high AI_{mod} and I_{Terr} (Tab. 2). Thus, brackish SPE-DOM retained and accumulated the terrestrial signal of streams. Brackish regions are not only zones of gradual mixing of different water masses (Van Dongen et al. 2008), where terrestrial-derived DOM of streams is exported to lakes and the ocean (Benner et al., 2004; Dittmar and Kattner, 2003; Ruediger, 2003) but are also zones of chemical transformation and uptake of riverine DOM, e.g. by flocculation and osmotrophy (Hoikkala et al. 2015). The relative increase of aromatic compounds in brackish SPE-DOM compared to stream SPE-DOM (Fig. 3) suggests a relative enrichment, for example, by selective degradation and oxidation of lower-molecular mass compounds in the wash of the waves as indicated by the increased CHO index and, I_{Deg} values (Fig. 5d) as shown for estuaries (Asmala et al., 2014). We conclude that the high molecular α-diversity in brackish samples represents both, the terrestrial input from streams mixing with the SPE-DOM signature of lake water and selective degradation of SPE-DOM in the high-energy wave zone.

Lake water differed in its SPE-DOM composition most strongly as compared to all other sample categories (Fig 7). Lake SPE-DOM was relatively enriched in unsaturated and saturated compounds,

485 which can include lipids and carbohydrates, but it was relatively depleted in aromatic and highly

486 unsaturated O-rich molecular formulae. Correspondingly, values of AI_{mod} and I_{Terr} decreased.

487 Photooxidation and microbial degradation can both remove aromatic DOM, such as lignin-derived

488 phenolics (Spencer et al. 2009; Helms et al. 2014; Vähätalo and Wetzel, 2004). Given the clear water

489 column and high irradiation at the TP (Wang et al., 2020), photooxidation can take place down to

490 greater depths in the lake. Hence, photooxidation in combination with microbial degradation can

491 explain the depletion of aromatic constituents when comparing brackish and lake SPE-DOM (blue

492 points in Fig. 6a and mass spectra in Fig. 6b).

493 In the estuary-lake gradient, riverine terrigenous SPE-DOM likely underwent a transformation, leaving

494 more recalcitrant SPE-DOM behind (Goldberg et al., 2015) as corroborated by relative increase of IOS

495 compounds compared to stream and brackish SPE-DOM, respectively (Table 2). Along with

496 transformation of imported riverine SPE-DOM, primary production in the lake plays a key role for the

497 SPE-DOM characteristics of Lake Nam Co. The increase in unsaturated (with and without N) compound

498 classes and the more negative CHO with lower molecular mass (Fig. 5e) in lake SPE-DOM (Fig. 3, yellow

499 points in Fig. 6a) act as indicators for bacterial and algal primary production in the lake. Microbial DOM

500 sources have been suggested for Lake Nam Co (Spencer et al., 2014; Maurischat et al., 2022) and other

501 large lakes of the TP (Liu et al., 2020). Performing a food web study in Lake Nam Co, Hu et al. (2016)

502 reported that mainly lake-borne organic carbon sources are utilised by zooplankton, showing the

503 importance of this type of DOM as substrate. The comparably low CHO index (Fig. 5e) underlines the

504 existence of low molecular mass reduced DOM produced in the lake, while higher molecular masses

505 of aromatic and highly unsaturated riverine origin are more oxidised in the lake environment compared

506 to other systems (indicated by the greatest steepness of the regression line in Fig. 5e), indicative of the

507 strong processing described above. Lake SPE-DOM exhibited sources derived from algal and microbial

508 production. Also, it was low in aromatic compounds and had lower terrigenous indices with a much

509 larger percentage of IOS compared to subcatchment streams SPE-DOM, suggesting more recalcitrant

510   compounds. The shift in SPE-DOM molecular composition, hence, shows that the terrigenous riverine

511   aromatic DOM is processed in the lake, while microbial DOM is produced.
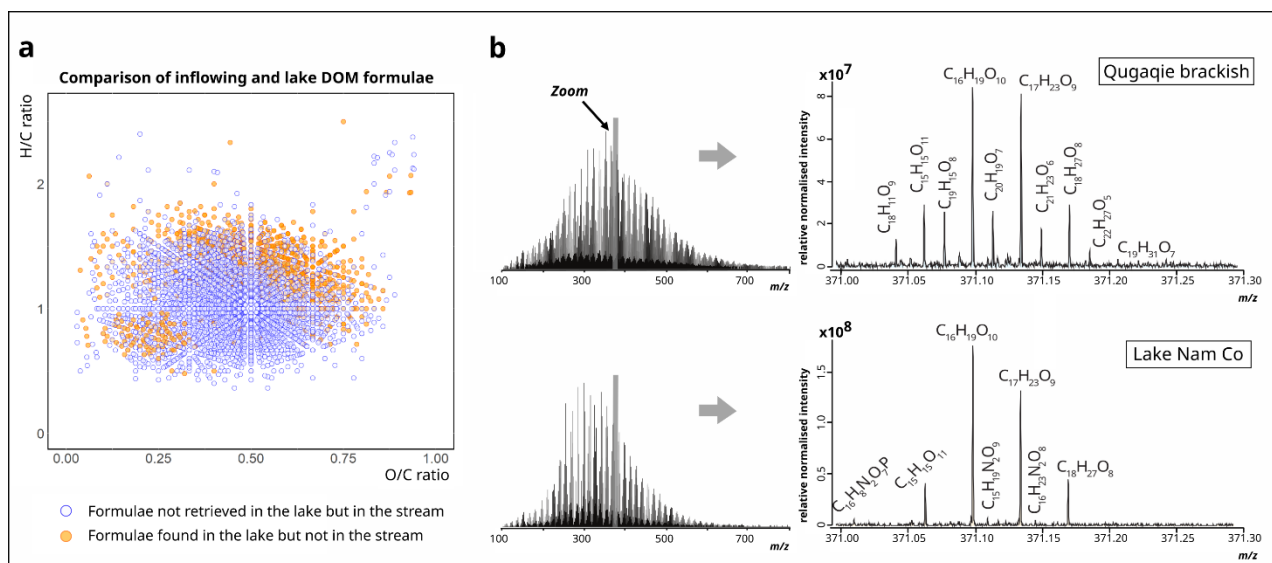
512   **Figure 6: A) van Krevelen diagram of molecular formulae retrieved in lake DOM but not in brackish**
513   **DOM and vice versa. B) Left: Intensity normalised overview mass spectra (m/z: 100-800) of Qugaqie**
514   **brackish DOM (Id 2:15) and a water sample from 30 m depth of the Lake Nam Co. Right: Exemplary**
515   **zoom into one mass range (371.0-371.3 *m/z*) of the respective samples. Note the axis scales shift.**

516

5. Conclusions

We elucidated the molecular composition and the processing of SPE-DOM in the High Asian endorheic Nam Co catchment. We investigated three subcatchments: *high glaciation, low glaciation, no glaciation / degraded*, including SPE-DOM samples of glaciers, groundwater springs, alpine wetlands, streams, the brackish mixing zone, and the weakly saline lake. The subcatchments differed in the molecular composition of SPE-DOM.

In the *high glaciation* catchment, we identified signatures of microbial, low-molecular mass SPE-DOM relatively enriched in S heteroatoms and unsaturated compounds with and without nitrogen, suggesting autotrophic sources in the glacial ice shield. Meanwhile, aromatic SPE-DOM with high abundance of highly unsaturated compounds, such as plant-derived lignin degradation products or polycondensed aromatics derived from the combustion of fossil fuels or household burning of yak faeces, hint at a depositional source by aeolian transport. The influence of glacial meltwater greatly modified SPE-DOM signatures along the *high glaciation* Qugaqie stream, probably delivering more bio-available compounds to the southern lake shoreline. The *low glaciation* Niyaqu subcatchment comprised a lower molecular α-diversity and had a mainly terrestrial-borne SPE-DOM source of highly unsaturated and aromatic compounds, attributed to the input of the surrounding *K. pygmaea* pastures to the streams. In comparison, spring SPE-DOM of the *degraded* Zhagu subcatchment was influenced by degradation of *K. pygmaea* pastures visible by highly degraded and oxidized signatures with a higher percentage of recalcitrant compounds. DOM signatures can thus be used to trace pasture degradation. Wetland SPE-DOM exhibited high molecular α-diversity and was relatively enriched with N-heteroatoms. Wetland SPE-DOM reflected the comparably high primary productivity of these systems. The reported degradation of alpine wetlands in High Asia can drive a large release of DOM to the streams; at Nam Co this can be considered a threat to the oligotrophic lake. The stream samples were mostly associated with the input of terrestrial-borne materials, originating from vascular plants and soils. These are attributed to the *K. pygmaea* ecosystem stretching along the paths of streams. From the pastures, aromatic and highly unsaturated SPE-DOM was constantly refuelled into the streams. Brackish SPE-DOM represented the mixing zone of stream and lake water. Here riverine terrestrial DOM entered the lake, indicating that DOM transformation along the stream was limited. However, lake SPE-DOM was different compared to the tributaries. Its molecular composition suggested photooxidation and microbial degradation as transformation of imported stream DOM, together with a source of microbial and algal production in the oligotrophic lake.

Our study shows that DOM cycling in the Nam Co catchment needs a thorough assessment, as it can be diverse on subcatchment level and between landscape units. In order to safeguard water resources and related ecosystem services, knowledge about the different sources and the fate of DOM is

indispensable. SPE-DOM molecular properties have proven to be selective for the source systems and hence allow to decipher landscape processes. In the case of the sensitive TP, they might be a way forward to better understand the local effects of global change.
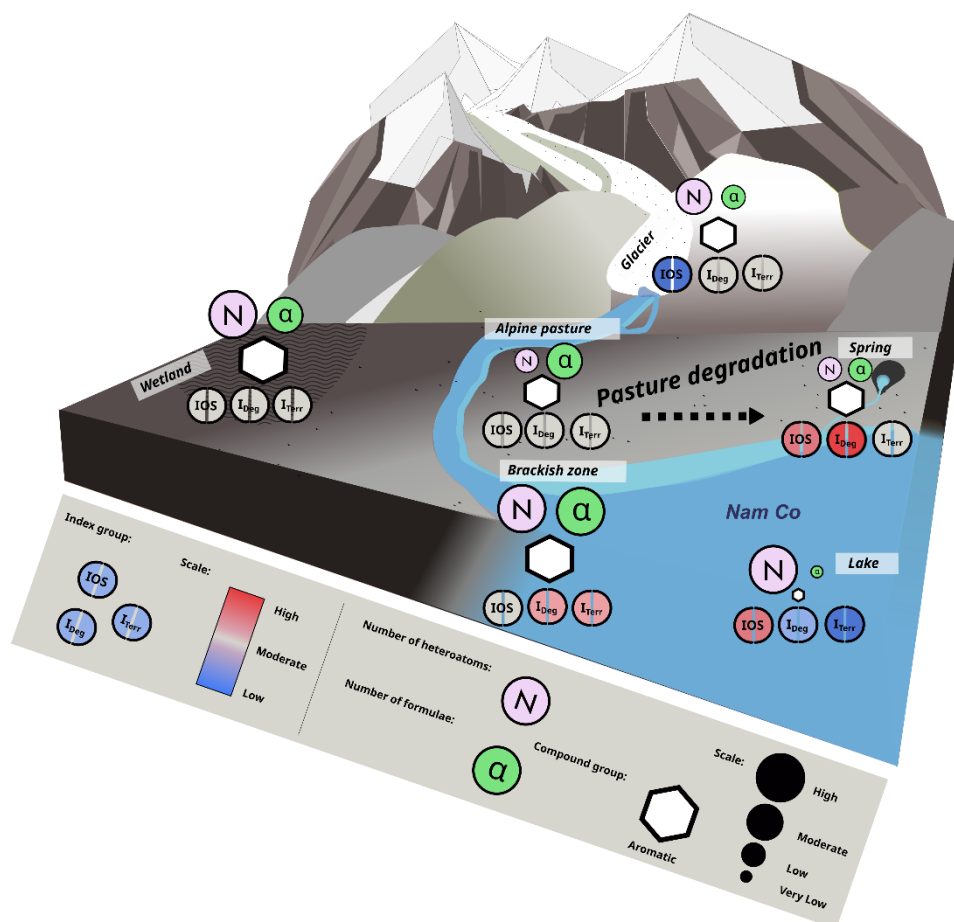
Figure 7: Overview of the molecular information from SPE-DOM along the water continuum of the TP. The number of N-heteroatoms is indicated relative to the total number of molecular formulae. The island of stability (IOS), degradation index (I_{Deg}), and terrestrial index (I_{Terr}) are ranging in a red-blue colour. Alpine steppe and groundwater spring samples are spatially correlated, and thus subject of a common evaluation. The local pasture degradation gradient is indicated by a dashed arrow.

Acknowledgements

The authors thank the staff of ITP-CAS and the NAMORS research station for their hospitality and assistance during the sampling campaign. We further thank the associated members of the TransTiP team for organizing the field work and helping hands during sampling.

This research is a contribution to the International Research Training Group "Geo-ecosystems in transition on the Tibetan Plateau (TransTiP)", funded by Deutsche Forschungsgemeinschaft (DFG grant 317513741 / GRK 2309).

M. Seidel is grateful for DFG funding within the Cluster of Excellence EXC 2077 "The Ocean Floor – Earth's Uncharted Interface" (Project number 390741603).

References

Adams H.E., Crump B.C., Kling G.W.: Temperature controls on aquatic bacterial production and community dynamics in arctic lakes and streams. Environmental microbiology,12,5,1319–33, 2010.

Adnan M., Kang S., Zhang G., Saifullah M., Anjum M.N., Ali A.F.: Simulation and Analysis of the Water Balance of the Nam Co Lake Using SWAT Model, Water, 11(7),2019a.

Adnan M., Kang S.C., Zhang G.S., Anjum M.N., Zaman M., Zhang Y.Q.: Evaluation of SWAT Model performance on glaciated and non-glaciated subbasins of Nam Co Lake, Southern Tibetan Plateau, China. J. Mt. Sci., 16, 5, 2019b.

Anesio A.M., Hodson A.J., Fritz A., Psenner R., Sattler B.: High microbial activity on glaciers: importance to the global carbon cycle. Global Change Biol., 15, 4, 2009.

Anslan S., Azizi Rad M., Buckel J., Echeverria Galindo P., Kai J., Kang W. et al.: Reviews and syntheses: How do abiotic and biotic processes respond to climatic variations in the Nam Co catchment (Tibetan Plateau)? Biogeosciences, 17, 5, 1261–79, 2020.

Asmala E., Autio R., Kaartokallio H., Stedmon C.A., Thomas D.N.: Processing of humic-rich riverine dissolved organic matter by estuarine bacteria: effects of predegradation and inorganic nutrients. Aquat Sci, 76, 3, 451–63, 2014.

Bandyopadhyay, J.: Securing the Himalayas as the Water Tower of Asia: An Environmental Perspective. Asia Policy 16, 2013.

Bai J., Ouyang H., Xiao R., Gao J., Gao H., Cui B. et al.: Spatial variability of soil carbon, nitrogen, and phosphorus content and storage in an alpine wetland in the Qinghai - Tibet Plateau, China. Soil Res.48, 8, 730, 2010.

Benner R., Benitez-Nelson B., Kaiser K., Amon R.M.W.: Export of young terrigenous dissolved organic carbon from rivers to the Arctic Ocean. Geophysical Research Letters, 31, 5, 2014.

Birnbaum Z.W.: On a use of the Mann-Whitney Statistic. In: Neyman J., Editor. Proceedings of the Third Berkeley Symposium on Mathematical Statistics and Probability: Held at the Statistical Laboratory, December 26-31, 1954. Berkeley, CA: University of California Press, 13–18, 1956.

Bolch T., Yao T., Kang S., Buchroithner M.F., Scherer D., Maussion F. et al.: A glacier inventory for the western Nyainqentanglha Range and the Nam Co Basin, Tibet, and glacier changes 1976–2009. The Cryosphere, 4, 3, 2010.

Bortz J., Schuster C..:Statistik für Human- und Sozialwissenschaftler: Limitierte Sonderausgabe. 7th ed. Berlin, Heidelberg, Springer, 2010.

Connolly C.T., Cardenas M.B., Burkart G.A., Spencer R.G.M., McClelland J.W.: Groundwater as a major source of dissolved organic matter to Arctic coastal waters. Nature communications, 11, 1, 2020.

D'Andrilli J., Junker J.R., Smith H.J. et al.: DOM composition alters ecosystem function during microbial processing of isolated sources. Biogeochemistry, 142, 281–298, 2019. https://doi.org/10.1007/s10533-018-00534-5.

Dexter E., Rollwagen-Bollens G., Bollens S.M.: The trouble with stress: A flexible method for the evaluation of nonmetric multidimensional scaling. Limnol. Oceanogr. Methods, 16, 7, 2018.

609 Dittmar T., Kattner G.: The biogeochemistry of the river and shelf ecosystem of the Arctic Ocean: a
610   review. Marine Chemistry, 83, 3-4, 2003.

611 Dittmar T., Koch B., Hertkorn N., Kattner G.: A simple and efficient method for the solid-phase
612   extraction of dissolved organic matter (SPE-DOM) from seawater. Limnol. Oceanogr. Methods, 6,
613   6, 2008.

614 Du Z., Wang X., Xiang J., Wu Y., Zhang B., Yan Y., et al.: Yak dung pat fragmentation affects its carbon
615   and nitrogen leaching in Northern Tibet, China. Agriculture, Ecosystems & Environment,
616   https://www.sciencedirect.com/science/article/pii/S0167880921000050, 2021.

617 Eklöf K., von Brömssen C., Amvrosiadi N., Fölster J., Wallin M.B., Bishop K.: Brownification on hold:
618   What traditional analyses miss in extended surface water records. Water Res., Vol. 203, 117544,
619   2010. https://doi.org/10.1016/j.watres.2021.117544.

620 Fahey Jr. G.C., Jung H.G.: Lignin as a Marker in Digestion Studies: a Review. Journal of Animal Science,
621   Vol. 57, 1, 1983.

622 Fellman J.B., Hood E., Spencer R.G.M.: Fluorescence spectroscopy opens new windows into dissolved
623   organic matter dynamics in freshwater ecosystems: A review, Limnol. and Oceanogr., 55, 2010.
624   DOI: 10.4319/lo.2010.55.6.2452

625 Flerus R., Lechtenfeld O.J., Koch B.P., McCallister S.L., Schmitt-Kopplin P., Benner R. et al.: A
626   molecular perspective on the ageing of marine dissolved organic matter. Biogeosciences, 9, 6,
627   1935–55, 2012.

628 Gao, J.: Wetland and Its Degradation in the Yellow River Source Zone. In: Brierley G., Li X., Cullum C.,
629   Gao J. (eds): Landscape and Ecosystem Diversity, Dynamics and Management in the Yellow River
630   Source Zone. Springer Geography. Springer, Cham. 2016.

631 Goldberg S.J., Ball G.I., Allen B.C., Schladow S.G., Simpson A.J., Masoom H., et al.: Refractory
632   dissolved organic nitrogen accumulation in high-elevation lakes. Nat Commun, 6, 6347, 2015.

633 Goodman K.J., Baker M.A., Wurtsbaugh W.A.: Lakes as buffers of stream dissolved organic matter
634   (DOM) variability: Temporal patterns of DOM characteristics in mountain stream-lake systems. J.
635   Geophys. Res., 116, 1, 2011.

636 Green N.W., McInnis D., Hertkorn N., Maurice P.A., Perdue E.M.: Suwannee River Natural Organic
637   Matter: Isolation of the 2R101N Reference Sample by Reverse Osmosis. Environmental
638   Engineering Science, 32, 1, 2015.

639 Green N.W., Perdue E.M., Aiken G.R., Butler K.D., Chen H., Dittmar T. et al.: An intercomparison of
640   three methods for the large-scale isolation of oceanic dissolved organic matter. Marine
641   Chemistry, 161, 2014.

642 Guo L. and Macdonald, R.W.: Source and transport of terrigenous organic matter in the upper Yukon
643   River: Evidence from isotope (δ13C, Δ14C, and δ15N) composition of dissolved, colloidal, and
644   particulate phases, Global Biogeochem. Cycles, 20, GB2011, 2006.

645 Harms T. K., Edmonds J. W., Genet H., Creed I. F., Aldred D., Balser A., Jones, J. B.: Catchment
646   influence on nitrate and dissolved organic matter in Alaskan streams across a latitudinal gradient,
647   *J. Geophys. Res. Biogeosci.*, 121, 350– 369, 2016.

648 Harris R.B.: Rangeland degradation on the Qinghai-Tibetan plateau: A review of the evidence of its
649   magnitude and causes, Journal of Arid Environments, 74, 1, 2010.

650 Hawkes J.A., D'Andrilli J., Agar J.N., Barrow M.P., Berg S.M., Catalán N. et al.: An international
651   laboratory comparison of dissolved organic matter composition by high resolution mass
652   spectrometry: Are we getting the same answer? Limnol. Oceanogr. Methods, 18, 6,2020.

653 Helms J.R., Mao J., Stubbins A., Schmidt-Rohr K., Spencer R.G.M., Hernes P.J. et al.: Loss of optical
654   and molecular indicators of terrigenous dissolved organic matter during long-term
655   photobleaching. Aquat Sci, 76, 3, 2014.

656 Hodson A., Anesio A.M., Tranter M., Fountain A., Osborn M., Priscu J. et al.: GLACIAL ECOSYSTEMS.
657   Ecological Monographs, 78, 1, 41–67, 2008.

658 Hoikkala L., Kortelainen P., Soinne H., Kuosa H.: Dissolved organic matter in the Baltic Sea. J. o.
659   Marine Systems, Vol. 142, 2015.

660 Hood E., Fellman J., Spencer R.G.M., Hernes P.J., Edwards R., D'Amore D. et al.: Glaciers as a source
661   of ancient and labile organic matter to the marine environment. Nature, 462, 7276, 1044–7,
662   2009.

663 Hopping, KA, Knapp, AK, Dorji, T, Klein, JA.: Warming and land use change concurrently erode
664   ecosystem services in Tibet. *Glob Change Biol*. 24, 2018.

665 Hu E., He H., Su Y., Jeppesen E., Liu Z.: Use of Multi-Carbon Sources by Zooplankton in an Oligotrophic
666   Lake in the Tibetan Plateau. Water, 8, 12, 2016.

667 Jolliffe I.T.: Principal Component Analysis. New York, NY: Springer-Verlag New York Inc; 2002.

668 Keil A., Berking J., Mügler I., Schütt B., Schwalb A., Steeb P.: Hydrological and geomorphological basin
669   and catchment characteristics of Lake Nam Co, South-Central Tibet. Quaternary International,
670   218, 1-2, 2010.

671 Kaiser K., Miehe G., Barthelmes A., Ehrmann O., Scharf A., Schult M., Schlütz F., Adamczyk S., Frenzel
672   B.: Turf-bearing topsoils on the central Tibetan Plateau, China: Pedology, botany, geochronology.
673   CATENA, 73, 3, 300-311, 2008.

674 Koch B.P., Dittmar T.: From mass to structure: an aromaticity index for high-resolution mass data of
675   natural organic matter. Rapid Commun. Mass Spectrom., 20, 5, 2006.

676 Koch B.P., Dittmar T.: From mass to structure: an aromaticity index for high-resolution mass data of
677   natural organic matter. Rapid Commun. Mass Spectrom., 30, 1, 2016.

678 Lechtenfeld O.J., Kattner G., Flerus R., McCallister S.L., Schmitt-Kopplin P., Koch B.P.: Molecular
679   transformation and degradation of refractory dissolved organic matter in the Atlantic and
680   Southern Ocean. Geochimica et Cosmochimica Acta, 126, 2, 321–37, 2014.

681 Leyva D., Jaffe R., Fernandez-Lima F.: Structural Characterization of Dissolved Organic Matter at the
682   Chemical Formula Level Using TIMS-FT-ICR MS/MS. Anal. Chem., 92, 17, 2020.

683 Li Y., Xiao K., Du J., Han B., Liu Q., Niu H. et al.: Spectroscopic fingerprints to track the fate of aquatic
684   organic matter along an alpine headstream on the Tibetan Plateau. The Science of the total
685   environment, 792, 148376, 2021.

686 Liu S., Schleuss P.-M., Kuzyakov Y.: Carbon and Nitrogen Losses from Soil Depend on Degradation of
687   Tibetan Kobresia Pastures. Land Degrad. Develop., 28, 4, 1253–62, 2017.

688 Liu S., He Z., Tang Z., Liu L., Hou J., Li T. et al.: Linking the molecular composition of autochthonous
689   dissolved organic matter to source identification for freshwater lake ecosystems by combination

690   of optical spectroscopy and FT-ICR-MS analysis. Science of The Total Environment,
691   https://www.sciencedirect.com/science/article/pii/S0048969719347552, 2020.

692 Lu Y., Li X., Mesfioui R., Bauer J.E., Chambers R.M., Canuel E.A. et al.: Use of ESI-FTICR-MS to
693   Characterize Dissolved Organic Matter in Headwater Streams Draining Forest-Dominated and
694   Pasture-Dominated Watersheds. PLOS ONE, 10, 12, 2015.

695 Ma W., Alhassan AR.M., Wang Y., Li G., Wang H., Zhao J.: Greenhouse gas emissions as influenced by
696   wetland vegetation degradation along a moisture gradient on the eastern Qinghai-Tibet Plateau
697   of North-West China. Nutr. Cycl. Agroecosyst., 112, 2018.

698 Mann B.F., Chen H., Herndon E.M., Chu R.K., Tolic N., Portier E.F. et al.: Indexing Permafrost Soil
699   Organic Matter Degradation Using High-Resolution Mass Spectrometry. PLOS ONE, 10, 6, 2015.

700 Maurischat P., Lehnert L., Zerres V.H.D., Tran T.V., Kalbitz K., Rinnan Å. et al.: The glacial-terrestrial-
701   fluvial pathway: A multiparametrical analysis of spatiotemporal dissolved organic matter
702   variation in three catchments of Lake Nam Co, Tibetan Plateau. The Science of the total
703   environment, 156542, 2022.

704 Medeiros P.M., Seidel M., Niggemann J., Spencer R.G.M., Hernes P.J., Yager P.L. et al.: A novel
705   molecular approach for tracing terrigenous dissolved organic matter into the deep ocean. Global
706   Biogeochem. Cycles, 30, 5, 689–99, 2016.

707 Merder J., Freund J.A., Feudel U., Hansen C.T., Hawkes J.A., Jacob B. et al.: ICBM-OCEAN: Processing
708   Ultrahigh-Resolution Mass Spectrometry Data of Complex Molecular Mixtures. Anal. Chem. 92,
709   10, 2020.

710 Miehe G., Miehe S., Kaiser K., Jianquan L., Zhao X.: Status and Dynamics of the Kobresia pygmaea
711   Ecosystem on the Tibetan Plateau. AMBIO: A Journal of the Human Environment, 37, 4, 2008.

712 Miehe G., Schleuss P-.M., Seeber E., Babel W., Biermann T., Braendle M. et al.: The Kobresia pygmaea
713   ecosystem of the Tibetan highlands - Origin, functioning and degradation of the world's largest
714   pastoral alpine ecosystem: Kobresia pastures of Tibet. The Science of the total environment, 648,
715   754–71, 2019.

716 Nieberding F., Wille C., Ma Y., Wang Y., Maurischat P., Lehnert L. et al.: Winter daytime warming and
717   shift in summer monsoon increase plant cover and net CO 2 uptake in a central Tibetan alpine
718   steppe ecosystem. J. Geophys. Res. Biogeosci, 2021.

719 Sankar M.S., Dash P., Lu Y. et al.: Land use and land cover control on the spatial variation of dissolved
720   organic matter across 41 lakes in Mississippi, USA. Hydrobiol., 847, 1159–1176, 2020.

721 Oksanen J., Blanchet F.G., Friendly M., Kindt R., Legendre P., McGlinn D. et al.: vegan: Community
722   Ecology Package, 2020.

723 Osterholz H., Turner S., Alakangas L.J., Tullborg E.-L., Dittmar T., Kalinowski B.E. et al.: Terrigenous
724   dissolved organic matter persists in the energy-limited deep groundwaters of the Fennoscandian
725   Shield. Nat Commun, 13, 1, 4837, 2022.

726 Pohlabeln A.M., Gomez-Saez G.V., Noriega-Ortega B.E., Dittmar T.: Experimental Evidence for Abiotic
727   Sulfurization of Marine Dissolved Organic Matter. Frontiers in Marine Science, 4,
728   http://dx.doi.org/10.3389/fmars.2017.00364, 2017.

729 Qiu, J.: China: The third pole. Nature 454, 2008.

730 Qu B., Zhang Y., Kang S., Sillanpää M.: Water quality in the Tibetan Plateau: Major ions and trace
731   elements in rivers of the "Water Tower of Asia". The Science of the total environment, 649, 571–
732   81, 2019.

733 R Core Team. R: A language and environment for statistical computing. Vienna, Austria: R Foundation
734   for Statistical Computing, 2013.

735 Riedel T., Dittmar T.: A method detection limit for the analysis of natural organic matter via Fourier
736   transform ion cyclotron resonance mass spectrometry. Anal. Chem., 86, 16, 2014.

737 Roebuck J.A., Seidel M., Dittmar T., Jaffé R.: Land Use Controls on the Spatial Variability of Dissolved
738   Black Carbon in a Subtropical Watershed. Environmental science & technology, 52, 15, 2018.

739 Roebuck J.A., Seidel M., Dittmar T., Jaffé R.: Controls of Land Use and the River Continuum Concept
740   on Dissolved Organic Matter Composition in an Anthropogenically Disturbed Subtropical
741   Watershed. Environmental science & technology, 54, 1, 2020.

742 Ruediger S.: Siberian River Run-Off in the Kara Sea: Characterisation, Quantification, Variability and
743   Environmental Significance, Elsevier, 2003.

744 Šantl-Temkiv T., Finster K., Dittmar T., Hansen B.M., Thyrhaug R., Nielsen N.W. et al.: Hailstones: a
745   window into the microbial and chemical inventory of a storm cloud. PLOS ONE, 8, 1, 2013.

746 Seidel M., Manecki M., Herlemann D.P.R., Deutsch B., Schulz-Bull D., Jürgens K. et al.: Composition
747   and Transformation of Dissolved Organic Matter in the Baltic Sea. Front. Earth Sci., 5, G01004,
748   2017.

749 Seidel M., Yager P.L., Ward N.D., Carpenter E.J., Gomes H.R., Krusche A.V. et al.: Molecular-level
750   changes of dissolved organic matter along the Amazon River-to-ocean continuum. Marine
751   Chemistry, 177, 2015.

752 Seifert A.-G., Roth V.-N., Dittmar T., Gleixner G., Breuer L., Houska T., et al.: Comparing molecular
753   composition of dissolved organic matter in soil and stream water: Influence of land use and
754   chemical characteristics. The Science of the total environment, 571, 2016.

755 Singer G.A., Fasching C., Wilhelm L., Niggemann J., Steier P., Dittmar T. et al.: Biogeochemically
756   diverse organic matter in Alpine glaciers and its downstream fate. Nature Geosci, 5, 10, 2012.

757 Spencer R.G.M., Guo W., Raymond P.A., Dittmar T., Hood E., Fellman J. et al.: Source and biolability
758   of ancient dissolved organic matter in glacier and lake ecosystems on the Tibetan Plateau.
759   Geochimica et Cosmochimica Acta, 142, 2014.

760 Spencer R.G.M., Stubbins A., Hernes P.J., Baker A., Mopper K., Aufdenkampe A.K. et al.:
761   Photochemical degradation of dissolved organic matter and dissolved lignin phenols from the
762   Congo River. J. Geophys. Res., 114, G3, 2009.

763 Telling J., Anesio A.M., Tranter M., Irvine-Fynn T., Hodson A., Butler C. et al.: Nitrogen fixation on
764   Arctic glaciers, Svalbard. J. Geophys. Res., 116, G3, 2011.

765 Thukral A.K.. A review on measurement of Alpha diversity in biology. Intern. Jour. Contemp.
766   Microbiol., 54, 1, 1, 2017.

767 Tran T.V., Buckel J., Maurischat P., Tang H., Yu Z., Hördt A. et al.: Delineation of a Quaternary Aquifer
768   Using Integrated Hydrogeological and Geophysical Estimation of Hydraulic Conductivity on the
769   Tibetan Plateau, China. Water, 13, 10, 2021.

770 van Dongen B.E., Zencak Z., Gustafsson Ö.: Differential transport and degradation of bulk organic
771   carbon and specific terrestrial biomarkers in the surface waters of a sub-arctic brackish bay
772   mixing zone. Marine Chemistry, 112, 3-4, 2008.

773 Vähätalo A.V., Wetzel R.G.: Photochemical and microbial decomposition of chromophoric dissolved
774   organic matter during long (months–years) exposures. Mar. Chem., Vol. 89, 1–4,313-326, 2004.

775 Wang H., Zhou X., Wan C., Fu H., Zhang F., Ren J.: Eco-environmental degradation in the northeastern
776   margin of the Qinghai–Tibetan Plateau and comprehensive ecological protection planning.
777   Environ. Geol. 55, 1135–1147, 2008.

778 Wang J., Huang L., Ju J., Daut G., Ma Q., Zhu L. et al.: Seasonal stratification of a deep, high-altitude,
779   dimictic lake: Nam Co, Tibetan Plateau. Journal of Hydrology, 584, 7, 2020.

780 Wang J., Zhu L., Daut G., Ju J., Lin X., Wang Y. et al.: Investigation of bathymetry and water quality of
781   Lake Nam Co, the largest lake on the central Tibetan Plateau, China. Limnology, 10, 2, 149–58,
782   2009.

783 Wang L., Zhang L., Cai W-J., Wang B., Yu Z.: Consumption of atmospheric CO_2 via chemical
784   weathering in the Yellow River basin: The Qinghai–Tibet Plateau is the main contributor to the
785   high dissolved inorganic carbon in the Yellow River. Chemical Geology, Vol. 430, 34-44, 2016.

786 Wickham H., Averick M., Bryan J., Chang W., McGowan L., François R. et al.: Welcome to the
787   Tidyverse. JOSS, 4, 43, 2019.

788 Wilson H.F., Xenopoulos M.A.: Effects of agricultural land use on the composition of fluvial dissolved
789   organic matter. Nature Geosci, 2, 1, https://www.nature.com/articles/ngeo391, 2009.

790 Wu X., Zhang W., Liu G., Yang X., Hu P., Chen T. et al.: Bacterial diversity in the foreland of the
791   Tianshan No. 1 glacier, China. Ann. Glaciol., 7, 1, 14038, 2012.

792 Yao T.: Tackling on environmental changes in Tibetan Plateau with focus on water, ecosystem and
793   adaptation. Sci. Bull. (Beijing). 64, 7, 417, 2019.

794 Yao T., Thompson L., Yang W. et al.: Different glacier status with atmospheric circulations in Tibetan
795   Plateau and surroundings. Nature Clim. Change 2, 2012.

796 Yoo H.-J., Choi Y.-J., Cho K.: Characterization of Natural Organic Matter in Spring Water. Mass
797   Spectrometry Letters, 11, 4, 2020.

798 Yu Z., Wu G., Li F., Chen M., Vi Tran T., Liu X. et al.: Glaciation enhanced chemical weathering in a cold
799   glacial catchment, western Nyaingêntanglha Mountains, central Tibetan Plateau. Journal of
800   Hydrology, 597, 5, 2021.

801 Zhang Y., Wang G., Wang Y.: Changes in alpine wetland ecosystems of the Qinghai–Tibetan plateau
802   from 1967 to 2004. Environ. Monit. Assess. 180, 189–199, 2011.

803 Zhang Z., Qin J., Sun H., Yang J., Liu Y.: Spatiotemporal Dynamics of Dissolved Organic Carbon and
804   Freshwater Browning in the Zoige Alpine Wetland, Northeastern Qinghai-Tibetan Plateau. Water,
805   12, 9, 2020.